Acta Cryst. (1989). A**45**, 699–703

Bloch-Wave Channeling and HOLZ Effects in High-Energy Electron Diffraction

BY L.-M. PENG* AND J. K. GJØNNES

Department of Physics, University of Oslo, 0316 *Oslo* 3, *Norway*

(*Received* 30 *November* 1988; *accepted* 15 *May* 1989)

Abstract

The circular arcs and high-order Laue zone (HOLZ) fine lines observed in both Kikuchi-line and convergent-beam electron diffraction (CBED) patterns have been shown to be consistent with the concept of Bloch-wave channeling of fast electrons along rows of atoms. This interpretation has the advantages that it provides a direct correlation between HOLZ lines and the crystal periodicity along the incident-beam direction, and forms a basis which could be incorporated into a more rigorous electron diffraction theory in the future for understanding the extreme Laue and Bragg cases of electron diffraction, as well as the intermediate reflection and transmission high-energy electron diffraction (RTHEED). Examples are given of all three types of CBED, RHEED and RTHEED patterns from Pt and GaAs single crystals, which show the common dynamical diffraction effects, circular arcs and HOLZ fine lines, resulting from Bloch-wave channeling.

1. Introduction

As first shown by Kikuchi & Nishikawa (1928) the diffraction of high-energy electrons by crystal cleavage surfaces contains a pattern of intersecting straight lines and bands in addition to the reflection spots. Shortly after, Shinohara (1932) observed that, as well as the straight lines, there exist circular arcs and parabolic curves. He explained the parabolas in the pattern as envelopes of the family of Kikuchi lines corresponding to a set of co-zonal planes and the circles as the boundaries inside which (excess) Kikuchi lines associated with a certain group of planes cannot appear. Sometimes these 'circles' are more like polygons, made up of enhanced segments of Kikuchi lines. In other cases the circles appear quite continuous and are separated from the nearest lines by a small gap, as shown for example by Emslie (1934) and Peng, Cowley &Yao (1988).

An alternative explanation for the circular lines was proposed by Emslie (1934). He suggested that, after some inelastic, or otherwise incoherent process, electrons could be confined to propagate along lines of atoms or 'tubes'. Diffraction from the one-dimensional periodicity along these tubes gives rise to cones of diffracted rays with the tube direction as axis. The circular Kikuchi lines arise as intersection of the cones with the photographic plate.

It is the purpose of this paper to present a generalization of Emslie's description of the circular lines and applications to convergent-beam electron diffraction (CBED) high-order Laue-zone (HOLZ) lines. The crystal periodicity in the directions perpendicular to the incident beam is included by treating the electron wavefunction inside the crystal in the Bloch-wave formalism. It is shown that the concept of Bloch-wave channeling along rows of atoms emerges, including the explanation of the circular arcs and HOLZ-line structure. The description is thus equivalent to that of HOLZ-line structure developed by Steeds & coworkers (Steeds, 1983). The description is applied to experimental patterns obtained in transmission, reflection and an intermediate case previously termed RTHEED by Peng & Cowley (1988).

2. Theory

As a starting point for the discussion, the propagation of electrons along lines of atoms in a crystal may be illustrated by the one-dimensional diagram Fig. 1. An electron wave traveling along the line of atoms will give rise to scattered wavelets emerging from each atom. These wavelets will interfere constructively in a direction lying in a set of conical surfaces with the line of atoms as axis and the semiangles θ of the cones given by

$$b/\lambda' - b\cos\theta/\lambda = n(\text{integer}). \qquad (1)$$

Here b is the atom spacing along the line, λ' is the wavelength in the space between the atoms, whereas λ is the wavelength outside that region. On neglecting relativistic effects we may write $\lambda = \lambda'(1+V/E)^{1/2}$, (1) is then reduced to

$$\cos\theta = (1 - n\lambda/b) + V/2E, \qquad (2)$$

where E is the accelerating voltage for the incident electrons and V an effective additional inner potential seen by the electron traveling along the row of atoms. An expression for the magnitude of this additional potential is derived below, by means of the Bloch-

* Now at: Department of Metallurgy and Science of Materials, University of Oxford, Parks Road, Oxford OX1 3PH, England.

0108-7673/89/100699-05$03.00

wave representation of the electron wavefield φ:

$$\varphi(\mathbf{r})=\sum_j \alpha^{(j)}\varphi^{(j)}(\mathbf{r}).$$

Each of the Bloch-wave $\varphi^{(j)}$ will see a potential which differs from the average potential V_0 by an effective additional potential given by the matrix element

$$V^{(j)}=\langle\varphi^{(j)}|V(\mathbf{r})-V_0|\varphi^{(j)}\rangle. \quad (3)$$

From the Fourier expansions of the Bloch wave

$$\varphi^{(j)}(\mathbf{r})=\sum_h C_h^{(j)}\exp\{i\mathbf{k}_h^{(j)}.\mathbf{r}\}$$

and of the crystal potential

$$V(\mathbf{r})-V_0=\sum_g{}' V_g\exp\{i\mathbf{g}.\mathbf{r}\},$$

the $V(j)$ are obtained in terms of the Fourier potentials:

$$V^{(j)}=\sum_h{}'\sum_g{}' V_{h-g}C_g^{(j)}C_h^{(j)*}. \quad (4)$$

We can manipulate this expression further by means of the fundamental equation

$$\{k_0^2-k_h^{(j)^2}\}C_h^{(j)}+\sum_g{}' v_{h-g}C_g^{(j)}=0 \quad (5)$$

and the usual approximation in the high-energy Laue case of electron diffraction:

$$k_0^2-k_h^{(j)^2}\simeq-2k_0(\gamma^{(j)}-S_h) \quad (6)$$

to obtain

$$V^{(j)}=2k_0\gamma^{(j)}-\sum_h|C_h^{(j)}|^2 2k_0S_h, \quad (7)$$

where $\gamma^{(j)}$ are the eigenvalues (*Anpassungen*) and S_h the excitation errors. Incidentally, (7) has the form of additional (negative) kinetic energy for Bloch wave *j*.

By substituting (7) into (2), we then obtain

$$\cos\theta^{(j)}=1-n\lambda/b+(k_0/E)\left\{\gamma^{(j)}-\sum_h|C_h^{(j)}|^2S_h\right\}, \quad (8)$$

where the last sum may be neglected, as a first approximation. Relativistic effects are readily included as a correction to the factor k_0/E, *viz*

$$\cos\theta^{(j)}=1-n\lambda/b+(k_0/E)(1+eE/2m_0C^2)\times\left\{\gamma^{(j)}-\sum_h|C_h^{(j)}|^2S_h\right\}. \quad (9)$$

Equations (8) and (9) relate the segments of the HOLZ ring to the strongly excited Bloch waves, *j*.

3. Observations and discussion

In Fig. 2, which is a reflection high-energy electron diffraction (RHEED) pattern taken from the (111) face of a Pt crystal with 100 keV electrons, a strong well defined circular Kikuchi line surrounded by a dark region is evident. The experiments were performed with a Philips EM-400T transmission electron microscope equipped with a double-tilt cold stage which allowed ±30 and ±15° tilt around the two axes. The vacuum of the microscope was 10^{-7} Torr (13 μPa). The sample was cooled to 192 K in order to reduce phonon scattering and reduce contamination.

The continuous circular Kikuchi line seen in this pattern is indeed suggestive of a description based on one-dimensional diffraction within rows of atoms. Very little evidence for interference between scattering in different [112] rows is seen in this inner circle, which by reference to (8) corresponds to the top branch of the dispersion surface. We may thus consider this part of the Kikuchi pattern in terms of wave packets which are localized around individual atom rows and hence with low potential energy, *i.e.* in a deeply bound state. Further away from the zone axis one sees a different pattern, which reveals the two-dimensional periodic structure normal to the atom

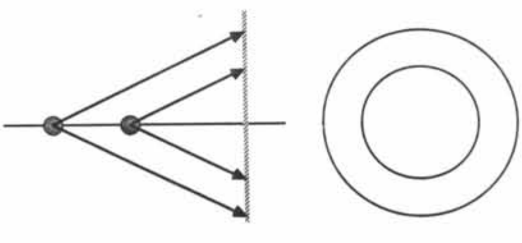

Fig. 1. Schematic diagram showing the formation of the circular lines in a diffraction pattern.

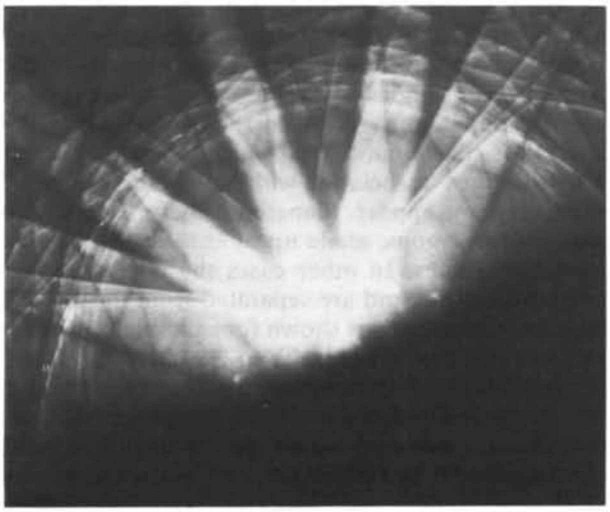

Fig. 2. RHEED pattern from a Pt (111) surface, with 100 keV incident beam along the [112] direction.

rows and eventually the usual straight-line Kikuchi pattern associated with the Bloch waves of high potential energy.

The CBED patterns Figs. 3 and 4, obtained in transmission from GaAs (111), are from a relatively thin region and a thicker region, respectively. The overall first impression from the pattern in Fig. 3 is of a double broken HOLZ ring, with roughly equal intensity on the inner and outer circle. Closer inspection shows finer details (see inset) and also that the

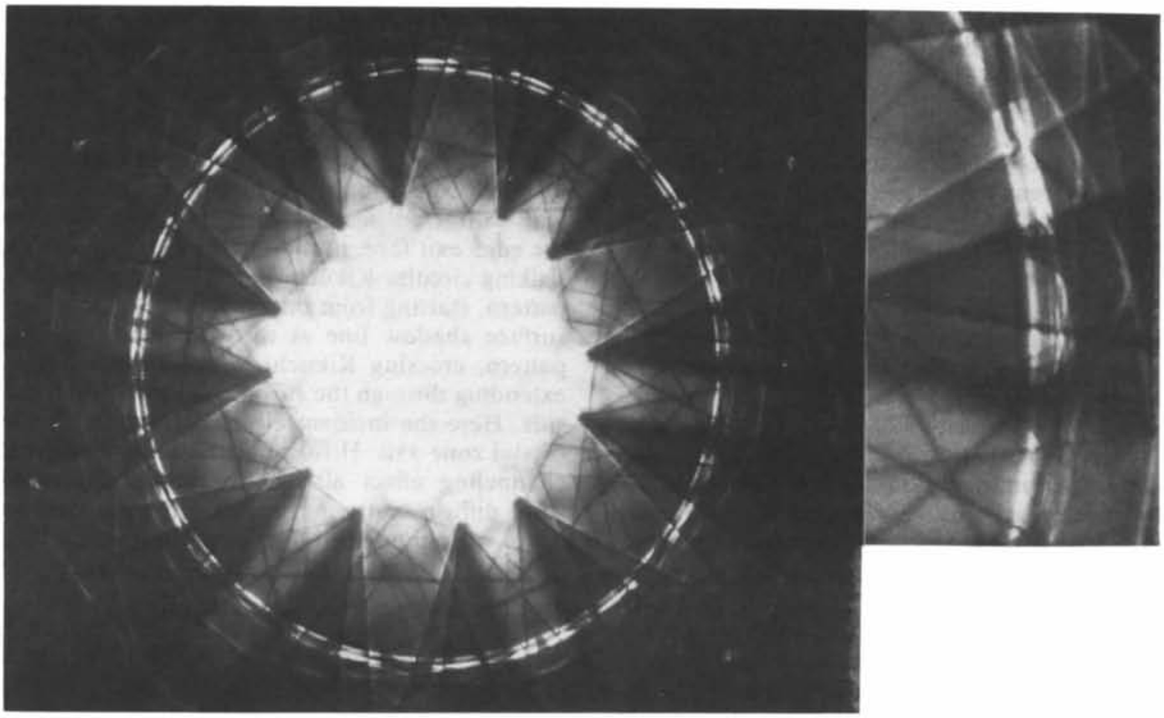

Fig. 3. CBED patterns from the ⟨111⟩ zone axis of a GaAs single crystal with 100 keV incident beam.

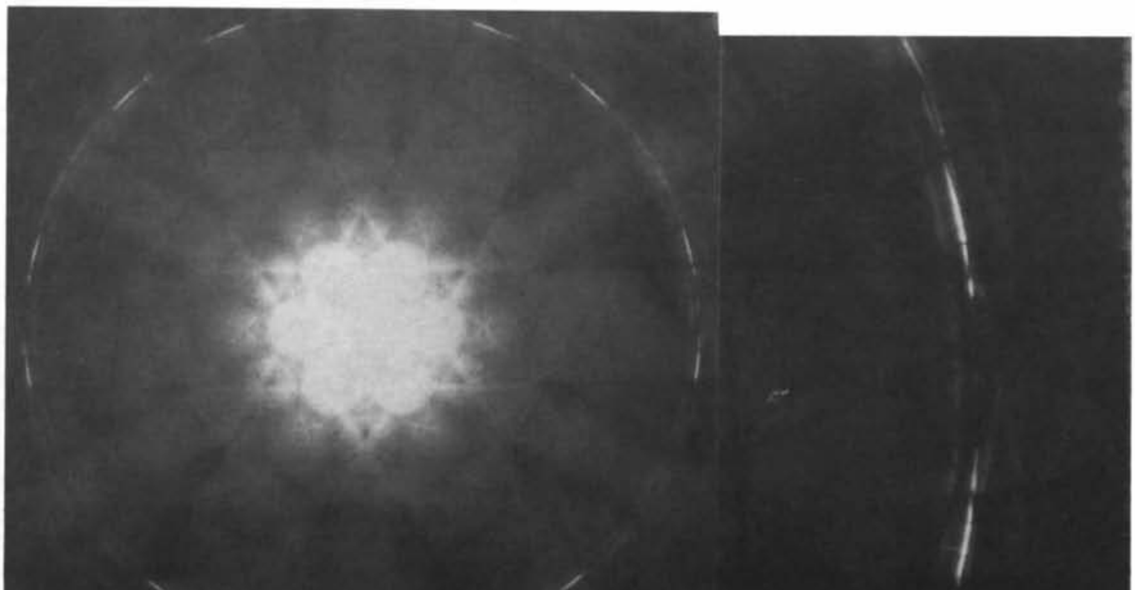

Fig. 4. Same as Fig. 3, but the pattern was obtained from a relatively thick region of the specimen.

ring which is closer to the zone axis is composed of segments which are smoother, with less orientation dependence of contrast than is found for the outer ring. The latter shows a more complicated contrast pattern, revealing stronger interactions with the straight Kikuchi lines associated with the three-dimensional periodic structure.

The gap between the two sets of lines indicates an energy difference of some tens of eV, which shows that the Bloch wave associated with the inner-line set is indeed strongly bound to the atom strings. However, interference effects which reveal coherence between different strings are clearly seen also from this ring. Outside the inner segments, especially within the weak HOLZ diffraction discs, many fine-line segments are noticed. According to the argument leading to (8), these are associated with different branches of the dispersion surface around the zone axis. The resolution of this fine structure is determined by the line width of the HOLZ lines. For relatively thin crystals this depends mainly on the crystal thickness, through the shape transform of the crystal along the incident-beam direction, see *e.g.* Cowley (1975). As the thickness is increased the line width will eventually be governed by the extinction length corresponding to the gap at the perturbed dispersion surface (Terasaki, Watanabe & Gjønnes, 1979). The resolution of the fine-line structure may thus be improved by increasing the specimen thickness.

As seen in Fig. 4, some improvement in HOLZ-line resolution is in fact achieved when the CBED pattern is taken from a thicker crystal. However, the intensity of many of the lines is also reduced, in particular the inner circular curve within each HOLZ disc. This is attributed to absorption effects associated with an imaginary addition $iV'(\mathbf{r})$ to the crystal potential $V(\mathbf{r})$. The introduction of $V'(\mathbf{r})$ to account for the inelastic and other diffuse scattering out of the Bragg beams is often referred to as the phenomenological theory of absorption. The salient effect in the present context is that different Bloch waves experience different absorption, usually described by an imaginary addition to the eigenvalue $\gamma^{(j)}$. This addition may be obtained in exactly the same manner as above, that is

$$V'^{(j)} = \langle \varphi^{(j)} | V'(\mathbf{r}) - V'_0 | \varphi^{(j)} \rangle.$$

It is often assumed that V' is proportional to V (notably after subtraction of the spatially averaged components V_0, V'_0). (See *e.g.* Gjønnes, Hafnor & Høier, 1971.)

It follows that the inner lines associated with a 'tightly bound Bloch wave', *i.e.* a large negative value of $V(j)$, will be strongly absorbed - as is expected from the fact that they have high density in the region around the atom column. It is a corollary to this high absorption that there will be strong diffuse scattering due to thermal motion and inner-shell excitations into the corresponding Kikuchi line, which is clearly noticed in the pattern in Fig. 4. These processes will contribute also within the CBED discs, and hence reduce some of the interference effects inside the discs.

An interesting experimental situation intermediate between the Laue and Bragg cases is provided by the so-called reflection and transmission high-energy electron diffraction (RTHEED), which was first explored by Peng & Cowley (1988). Such a pattern, obtained by focusing the incident electron beam near the edge of an atomically flat GaAs (110) surface is shown in Fig. 5. The resonance beam corresponding to channeling along the surface is shown together with diffracted beams which have escaped through the edge exit face, normal to the entrance surface. A striking circular Kikuchi line is observed also in this pattern, starting from the reflection region above the surface shadow line at the right-hand side of the pattern, crossing Kikuchi lines and envelopes and extending through the surface shadow onto the other side. Here the incident electron beam is far from a crystal zone axis. However, the circular arc reveals a channeling effect also here, presumably resulting from diffuse scattering into Bloch-wave channeling states with high density at an atom row.

4. Concluding remarks

The present description of HOLZ-line fine structure in terms of Bloch-wave channeling along zone axes

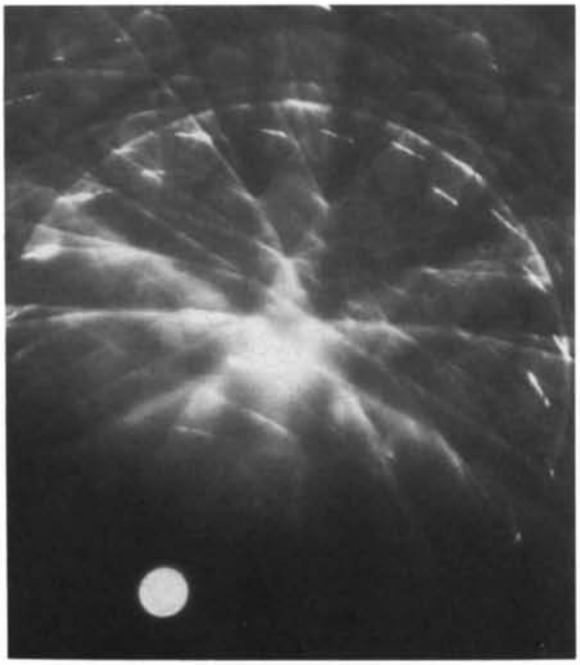

Fig. 5. RTHEED pattern from GaAs single crystal with 100 keV incident electron beam. This pattern shows a striking circular Kikuchi line extending from the reflection region to the transmission region.

incorporates the old idea by Emslie (1934) based on propagation of electrons along atom strings. HOLZ rings of circular shape are thus related to the repetition b along the zone axis - as would be the case for individual strings. The potential at the string, *cf.* (2), is interpreted as the potential $V(j)$ seen by a strongly excited Bloch wave. The resulting increment in wavelength is related to the (negative) increment in wave vector given by the eigenvalue $\gamma^{(j)}$ [(7)] through the kinetic energy. The circular rings correspond to Bloch waves with low potential energy, located near the atom strings, sometimes called 'tightly bound'. Bloch waves with higher potential energy will usually display more interference effects associated with interference between scattering in different strings and the typical HOLZ-line fine structure consisting of curved or straight Kikuchi- or Kossel-line segments. Our description is equivalent to the theory developed by Steeds & co-workers (Steeds, 1983).

The description is seen to apply to experimental patterns taken in reflection as well as in transmission and in intermediate configurations, including CBED patterns and channeling appearing in Kikuchi pattern and surface channeling.

We thank Professor J. M. Cowley for many valuable discussions. Part of the work was supported by NSF grant DMR-8510059 and made use of the resources of the ASU Facility for High Energy Electron Microscopy, supported by NSF grant DMR-8611609.

References

COWLEY, J. M. (1975). *Diffraction Physics.* Amsterdam: North-Holland.
EMSLIE, A. G. (1934). *Phys. Rev.* **45**, 43-46.
GJØNNES, J., HAFNOR, O. A. & HØIER, R. (1971). *Jernkontorets Ann.* **155**, 471-472.
KIKUCHI, S. & NISHIKAWA, S. (1928). *Proc. Imp. Acad. (Tokyo)*, **4**, 475.
PENG, L.-M. & COWLEY, J. M. (1988). *Surf. Sci.* **201**, 559-572.
PENG, L.-M., COWLEY, J. M. & YAO, N. (1988). *Ultramicroscopy*, **26**, 189-194
SHINOHARA, K. (1932). *Sci. Pap. Inst. Phys. Chem. Res. (Jpn)*, **20**, 39.
STEEDS, J. M. (1983). In *Quantitative Electron Microscopy*, edited by J. N. CHAPMAN & A. J. CRAVEN. Scottish Univ. Summer School in Physics, Edinburgh, Scotland.
TERASAKI, O., WATANABE, D. & GJØNNES, J. (1979). In Proc. Fifth Int. Conf. on High-Voltage Electron Microscopy, p. 263.

Acta Cryst. (1989). A**45**, 703-708

Determination of the Enantiomorph from Intensity Measurements of Three-Beam Bragg-Surface Diffraction of X-rays

BY SHIH-SEN CHIEN, MAU-TSU TANG AND SHIH-LIN CHANG*

Department of Physics, National Tsing-Hua University, Hsinchu, Taiwan 30043

(*Received* 27 *December* 1988; *accepted* 15 *May* 1989)

Abstract

An analytical expression for the intrinsic peak width of three-beam Bragg diffraction involving a surface reflection is derived on the basis of the dynamical theory of X-ray diffraction. Utilization of this expression in peak intensity measurements is proved to lead to direct determination of the enantiomorph of the triplet structure-factor invariant involved in a three-beam Bragg-surface diffraction. Effects of polarization on the kinematical peak intensity and on the intrinsic peak width are also discussed.

1. Introduction

The use of X-ray multiple diffraction for phase determination has long been proposed (Lipscomb, 1949). Investigations on the possibilities of extracting phase information from the intensity variation near or at the exact multi-beam diffraction position have been intensively pursued in recent years. These include the work reported by Hart & Lang (1961), Ewald & Héno (1968), Colella (1974), Post (1977), Jagodzinski (1980), Chapman, Yoder & Collella (1981), Chang (1981, 1982), Høier & Aanestad (1981), Juretschke (1982*a*, *b*), Hümmer & Billy (1982, 1986), Høier & Marthinsen (1983), Post, Nicolosi & Ladell (1984), Chang (1986, 1987), Shen (1986), Thorkildsen (1987), Mo, Haubach & Thorkildsen (1988), Shen & Colella (1988) and many others.

Recently, quantitative determination of the phases of structure-factor triplets using intensity profiles of three-beam (a primary, a secondary and an incident beam) diffraction has been demonstrated by Chang & Tang (1988) and Tang & Chang (1988). In that discussion, Bragg-Laue and Bragg-Bragg types of

* To whom all correspondence should be addressed.

0108-7673/89/100703-06$03.00